

# A comparative study on hydrogenation of carbon dioxide and carbon monoxide over iron catalyst

Hisanori Ando <sup>\*</sup>, Yasuyuki Matsumura <sup>1</sup>, Yoshie Souma

*Osaka National Research Institute, AIST, Midorigaoka, Ikeda, Osaka 563-8577, Japan*

Received 22 June 1999; received in revised form 9 August 1999; accepted 13 September 1999

## Abstract

Hydrogenation of CO<sub>2</sub> to hydrocarbons over iron catalysts reduced with hydrogen at 350°C and 500°C has been compared with that of CO. The space time yield of hydrocarbons from CO<sub>2</sub> at 250°C is significantly lower than from CO and the selectivity to olefin compounds is also lower from CO<sub>2</sub>. During the reaction with CO,  $\chi$ -Fe<sub>2.2</sub>C is formed, and the surface, which is oxidized even after the reduction at 500°C, is further reduced. On the other hand, formation of the carbide species is slight in hydrogenation of CO<sub>2</sub> while the surface is rather oxidized. The formation of the carbide species, which is probably the active site of hydrocarbon formation, is suppressed in the presence of CO<sub>2</sub>. © 2000 Elsevier Science B.V. All rights reserved.

*Keywords:* Carbon monoxide; Carbon dioxide; Hydrogenation; Comparative study; Iron catalyst; XRD; XPS

## 1. Introduction

Iron-based catalysts are usually employed in the hydrogenation of CO to hydrocarbons and oxygenated products (Fischer–Tropsch synthesis) [1–9]. The active phase of the reaction is believed to be the iron carbide species, while the contribution of other phases such as metallic iron has yet to be cleared. Miller and Moskovits showed a different pathway for the formation of oxygenates and this implies the presence of other

active phases [10]. However, identification of the active phase is not easy because the surface of iron is not stable during the reaction. That is, formation of carbide species accompanies accumulation of carbon on the surface. In case of Fe<sub>2</sub>O<sub>3</sub>, which is often used as a catalyst precursor, reduction of the oxide to Fe<sub>3</sub>O<sub>4</sub> and metallic iron also proceeds [5].

Iron catalysts are also active in the hydrogenation of CO<sub>2</sub> [11–15]. The hydrogenation can be understood as sequential reaction of reduction of CO<sub>2</sub> to CO and hydrogenation of CO. However, some dissimilarity from CO hydrogenation was reported [16]. Dwyer and Somorjai compared the reactions from CO and CO<sub>2</sub> over iron foil, and they showed less hydrocarbon-chain growth and higher specific methanation rate in CO<sub>2</sub> hydrogenation [9].

<sup>\*</sup> Corresponding author. Tel.: +81-727-51-9652; fax: +81-727-51-9629.

*E-mail address:* h-ando@onri.go.jp (H. Ando).

<sup>1</sup> Present address: Research Institute of Innovative Technology for the Earth, Kizugawadai, Kizu, Kyoto 619-0292, Japan. Tel.: +81-774-75-2305; fax: +81-774-75-2318.

In the present study we have compared the activation process in the hydrogenation of CO and CO<sub>2</sub> over iron catalysts in order to avoid excessive carbide formation. This formation proceeds in the reaction for a long period and has characterized the active sites of the reactions with CO and CO<sub>2</sub>, which are always by-products in the Fischer–Tropsch reaction.

## 2. Experimental

### 2.1. Catalyst preparation

Iron oxide was prepared by precipitation from an aqueous solution of Fe(NO<sub>3</sub>)<sub>3</sub> (1 M) with NH<sub>4</sub>OH (1 M) at 70°C. After being stirred at room temperature for 12 h, the precipitate was filtrated, dried at 120°C for 6 h, and calcined in air at 500°C for 5 h. The resulting solid was crushed into granules of less than 60 mesh.

### 2.2. Reaction procedure

The hydrogenation of carbon oxides was carried out with a fixed-bed flow reactor made of stainless steel tube with 10-mm i.d. A catalyst was pretreated with a hydrogen stream (10 vol.%) diluted with nitrogen under atmospheric pressure at 350°C or 500°C for 12 h. After introduction of a reactant mixture (33% CO in H<sub>2</sub> or 25% CO<sub>2</sub> in H<sub>2</sub>) at room temperature, the pressure was raised to 1 MPa and the temperature was set at 250°C. The effluent gas was analyzed with on-line gas chromatographs of whose columns were Porapak Q for CO<sub>2</sub>, MS-13X for methane and CO, PLOT column (fused silica, Al<sub>2</sub>O<sub>3</sub>/KCl) for hydrocarbons, and PEG-6000 (15%) + TCEP (8%) supported on Chromosorb WAW (60/80 mesh) for alcohols. Yields and selectivities were calculated based on carbon numbers in the products.

### 2.3. Characterization of the catalyst

The BET surface areas of the catalysts were determined from the isotherms of nitrogen

physisorption. X-ray diffraction (XRD) patterns were recorded with a Rigaku ROTAFLEX diffractometer (Cu-K $\alpha$ ). The mean crystallite size of the catalyst was estimated from the peak width using the equation of Scherrer [17]. Surface analyses by X-ray photoelectron spectroscopy (XPS) were performed with a Shimadzu ESCA-750. The spectra were recorded after argon-ion sputtering for 1 min (2 kV, 25 mA). The binding energy was corrected with the energy of C(1s) (284.6 eV) for carbon contaminant [18].

## 3. Results

### 3.1. Hydrogenation of CO

Hydrogenation of CO was carried out over iron catalyst reduced at 500°C. Conversion of CO increased in the initial stage of the reaction and it was mostly stabilized after 5 h-on-stream (Fig. 1, solid symbols). The major products were C<sub>1</sub>–C<sub>9</sub> hydrocarbons, C<sub>1</sub>–C<sub>3</sub> alcohols, and CO<sub>2</sub>. Over the catalyst reduced at 350°C, the catalyst was activated sooner than that pretreated at 500°C while the activities after the activation process were very similar (Fig. 1, open symbols).

In general, waxes and other heavy products formed in the reaction accumulate in catalyst pores, and they rather deactivates the catalyst [2]. Under the present reaction conditions, few

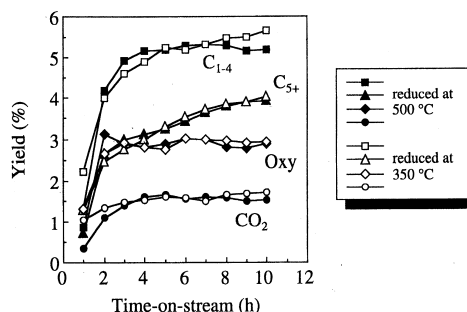


Fig. 1. Hydrogenation of CO at 250°C over iron catalyst. Open symbols, reduced at 350°C; solid symbols, reduced at 500°C. F/W, 9000 ml g<sup>-1</sup> h<sup>-1</sup>.

Table 1

Catalytic activity of iron catalyst on the olefin content and the yield of alcohols with different reduction temperatures

Reaction conditions: temperature, 250°C; pressure, 1 MPa; time-on-stream, 10 h.

Reactant (F/W) <sup>a</sup>	Reduction temperature (°C)	Olefin/(olefin + paraffin)			Yield (%)			BET surface area <sup>b</sup> (m <sup>2</sup> g <sup>-1</sup> )
		C <sub>2</sub>	C <sub>3</sub>	C <sub>4</sub>	MeOH	EtOH	PrOH	
CO/H <sub>2</sub> (9000)	500	0.259	0.668	0.661	1.68	0.86	0.33	1.8
CO/H <sub>2</sub> (9000)	350	0.176	0.564	0.574	1.67	0.92	0.35	1.5
CO <sub>2</sub> /H <sub>2</sub> (1200)	500	0.010	0.029	0.028	1.18	0.19	– <sup>c</sup>	2.2
CO <sub>2</sub> /H <sub>2</sub> (1200)	350	0.012	0.048	0.060	1.13	0.15	– <sup>c</sup>	2.1

<sup>a</sup> ml g-cat<sup>-1</sup> h<sup>-1</sup>.<sup>b</sup> After reaction.<sup>c</sup> Not detected.

heavy products were detected and no significant deactivation was observed after 10 h-on-stream, while the mass balance was always more than 95%. The BET surface areas were 3.5 and 4.5 m<sup>2</sup> g<sup>-1</sup> for the samples just after the reduction at 500°C and 350°C, respectively, and they decreased to 1.8 and 1.5 m<sup>2</sup> g<sup>-1</sup>, respectively, after the reaction (Table 1).

The product distributions of hydrocarbons after 10 h-on-stream mostly obeyed the Schulz–Flory's law as shown in Fig. 2. From the slope of the plots, the logarithms of probability of chain growth,  $\ln \alpha$ , were obtained as  $-0.38$  and  $-0.37$  for the catalysts reduced at 350°C and 500°C, respectively. The catalyst reduced at 350°C produced appreciably lower selectivities to olefins (C<sub>2–4</sub>) than that reduced at 500°C (see Table 1). No significant difference was

observed in the yields of alcohols between these catalysts.

### 3.2. Hydrogenation of CO<sub>2</sub>

When CO<sub>2</sub> was a reactant, the activation process was slow and the catalytic activity still increased with time-on-stream even after 5 h (Fig. 3). The space–time–yield was significantly low compared with the CO hydrogenation, e.g., the values for methane at 10 h-on-stream were 0.4 mmol g<sup>-1</sup> h<sup>-1</sup> and 2 mmol g<sup>-1</sup> h<sup>-1</sup> for CO<sub>2</sub> and CO conversions over the catalyst reduced at 500°C, respectively. After 1 h-on-stream, the activity of the catalyst reduced at 350°C was very small while no obvious difference in activity was present between the catalysts pretreated at 350°C and 500°C after 10 h-on-stream. The selectivities to olefins were

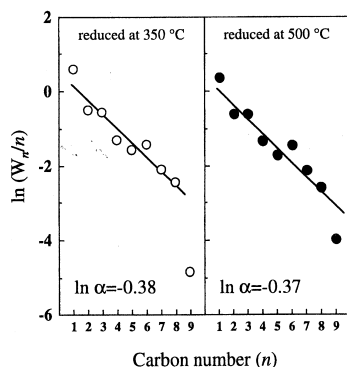


Fig. 2. Schulz–Flory plots for the hydrogenation of CO over iron catalyst. Open symbols, reduced at 350°C; solid symbols, reduced at 500°C.

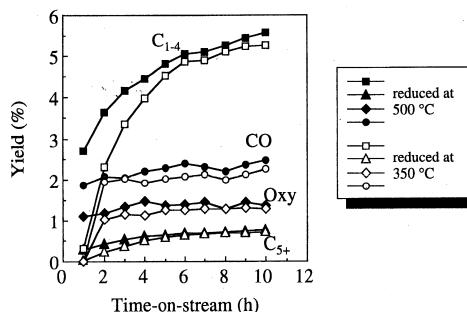


Fig. 3. Hydrogenation of CO<sub>2</sub> at 250°C over iron catalyst. Open symbols, reduced at 350°C; solid symbols, reduced at 500°C. F/W, 1200 ml g-cat<sup>-1</sup> h<sup>-1</sup>.

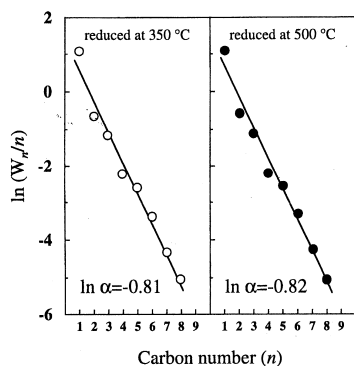


Fig. 4. Schulz–Flory plots for the hydrogenation of  $\text{CO}_2$  over iron catalyst: open symbols, reduced at  $350^\circ\text{C}$ ; solid symbols, reduced at  $500^\circ\text{C}$ .

very small and methanol was mainly produced as oxygenate (see Table 1). The distribution of hydrocarbons was also followed by the

Schulz–Flory's law but the values of  $\ln \alpha$  were  $-0.81$  and  $-0.82$  for the catalysts reduced at  $350^\circ\text{C}$  and  $500^\circ\text{C}$ , respectively (Fig. 4).

### 3.3. XRD measurements

XRD analyses were performed with the iron catalysts. A clear peak at  $44.5^\circ$  attributed to  $\alpha\text{-Fe}$  was found for the catalyst taken out of reactor just after the pre-reduction at  $500^\circ\text{C}$ , while a slight peak attributed to  $\text{Fe}_3\text{O}_4$  was also present at  $35.3^\circ$  in  $2\theta$  (Fig. 5a) [19]. The mean crystallite size of  $\alpha\text{-Fe}$  in the sample just after the pretreatment was estimated to be 65 nm from the XRD peak at  $44.5^\circ$ . The catalyst taken out of the reactor after the reaction with  $\text{CO}$  kept the structure of  $\alpha\text{-Fe}$  and small peaks

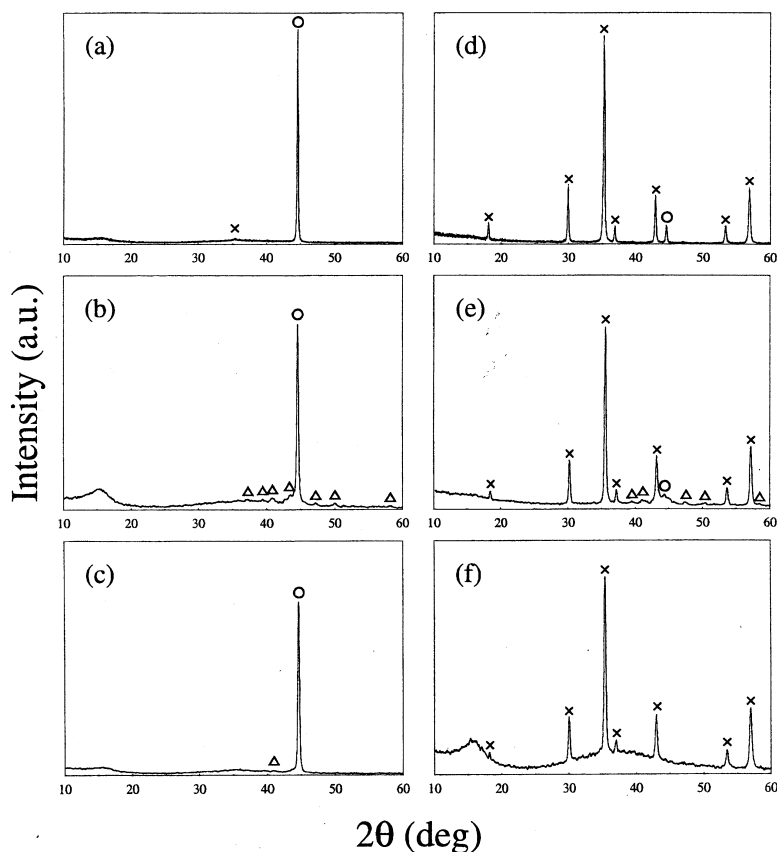


Fig. 5. XRD patterns for iron catalysts: (O) Fe; (X)  $\text{Fe}_3\text{O}_4$ ; ( $\Delta$ )  $\text{Fe}_{2.2}\text{C}$ : (a) just after reduction at  $500^\circ\text{C}$ ; (b) followed by reaction with  $\text{CO}$ ; (c) followed by reaction with  $\text{CO}_2$ ; (d) just after reduction at  $350^\circ\text{C}$ ; (e) followed by reaction with  $\text{CO}$ ; (f) followed by reaction with  $\text{CO}_2$ .

attributed to  $\chi$ -Fe<sub>2.2</sub>C were also found (Fig. 5b) [3]. No significant change in the crystallite size of  $\alpha$ -Fe was detected. After CO<sub>2</sub> hydrogenation, a very slight peak at 41.8° was recorded with a main peak attributed to  $\alpha$ -Fe (Fig. 5c). The peaks attributed to  $\alpha$ -Fe and Fe<sub>3</sub>O<sub>4</sub> were seen in the pattern of catalysts just after being reduced at 350°C (Fig. 5d). The peaks of  $\chi$ -Fe<sub>2.2</sub>C were also recorded with the sample reduced at 350°C after the reaction with CO (Fig. 5e). On the other hand, only peaks attributed to Fe<sub>3</sub>O<sub>4</sub> were recorded after the reaction with CO<sub>2</sub> (Fig. 5f).

In the cases of the catalysts used in CO<sub>2</sub> hydrogenation, no peaks attributed to the carbide species nor metallic iron phase were recorded (Fig. 5e and f). No significant change in the structure was detected for the catalysts reduced at 350°C or 500°C.

### 3.4. Surface analyses by XPS

Although the XRD analyses did not show a clear change in the structure of the catalyst except for the formation of carbide species during the hydrogenation of CO, a change in the oxidation state of the surface iron was detected by recording XPS of the catalysts. The sample was taken out from the reactor and transferred into XPS instrument in air, but it was confirmed that the exposure of samples to air is not a serious drawback in the reliable characterization of the catalyst [5,20]. In the range of Fe 2p<sub>3/2</sub> a major peak attributed to Fe[0] was recorded at 706.9 eV in the XPS for the catalyst, just after the reduction at 500°C (Fig. 6a) [18]. The spectrum can be deconvoluted to three Gaussian peaks, and minor peaks were at 709.5 and 712.6 eV. The former can be attributed to Fe(II) and the latter to Fe(III) [18]. After the reaction with CO, the peak at 706.9 eV was intensified (Fig. 6b). However, in the case of the reaction with CO<sub>2</sub>, the peak became small and both peaks at 709.5 and 712.6 eV were mainly present (Fig. 6c).

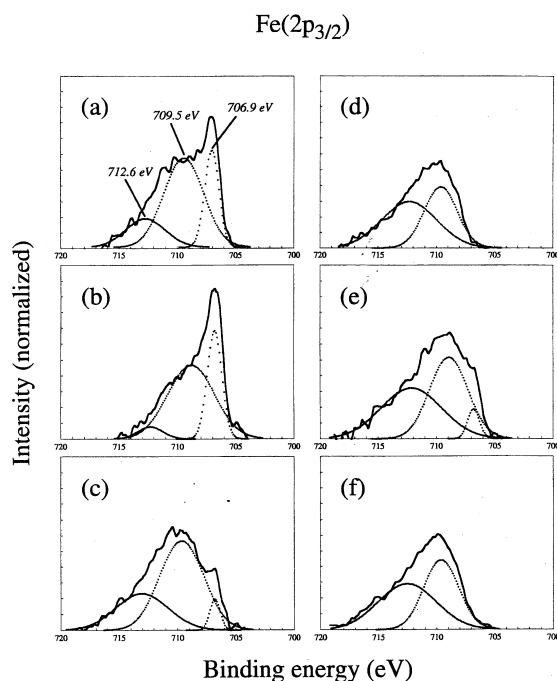


Fig. 6. XPS spectra of Fe(2p<sub>3/2</sub>) for iron catalysts: (a) just after reduction at 500°C; (b) followed by reaction with CO; (c) followed by reaction with CO<sub>2</sub>; (d) just after reduction at 350°C; (e) followed by reaction with CO; (f) followed by reaction with CO<sub>2</sub>.

After the reduction at 350°C the peak at 706.9 eV was not recorded (Fig. 6d), but a small peak at 706.9 eV, attributed to metallic species, was seen in the XPS after the following reaction with CO (Fig. 6e). The XPS profile after the reaction with CO<sub>2</sub> was similar to the one taken just after the pretreatment at 350°C (Fig. 6f).

## 4. Discussion

In the reactions with CO, no significant change in the activity can be seen with the iron catalysts pretreated at different temperatures except in the initial stage of the reaction (see Fig. 1). Dictor and Bell reported that Fe<sub>2</sub>O<sub>3</sub> is slowly activated in the initial stage of the Fischer–Tropsch synthesis [3]. However, in the case of the catalyst reduced at 350°C, of which the major structure is Fe<sub>3</sub>O<sub>4</sub>, the activation process

is rather quick compared with that pretreated at 500°C. Reymond et al. showed formation of  $\chi$ -Fe<sub>2.2</sub>C accompanied with the reduction of Fe<sub>2</sub>O<sub>3</sub> to Fe<sub>3</sub>O<sub>4</sub> during the reaction [5]. It is a general understanding that iron carbides on the surface are active species of Fischer–Tropsch reaction, and the carbide species can be observed in the XRD pattern of both the used iron catalysts reduced at 350°C and at 500°C. Hence, Fe<sub>3</sub>O<sub>4</sub> is an active precursor as well as metallic iron while inactive carbide is often formed on the metal [5].

Iron is known as the catalyst for the water gas shift (WGS) reaction. In order to evaluate the contribution of the WGS reaction to CO hydrogenation, the value of  $K_p$  which is equal to  $P(\text{CO}_2)P(\text{H}_2)/P(\text{CO})P(\text{H}_2\text{O})$  was calculated, where  $P(i)$  represents a partial pressure of a component  $i$ . The partial pressure of each component was estimated from the product distribution. The equilibrium value of the WGS reaction at 250°C is 56 and both values of  $K_p$  for the CO hydrogenation over the catalysts reduced at 350°C and 500°C after 10 h-on-stream were only 0.4. On the other hand, a reverse WGS reaction took place in the CO<sub>2</sub> hydrogenation and the values of  $1/K_p$  for the reaction over the catalysts reduced at 350°C and 500°C were calculated as  $(0.1\text{--}0.2) \times 10^{-2}$ , while the equilibrium value is  $1.8 \times 10^{-2}$ . This suggests that the formation rate of CO is fairly small under the reaction conditions.

Although Dewyer and Somorjai reported a higher methanation rate from CO<sub>2</sub> and H<sub>2</sub> over iron foils than that from CO and H<sub>2</sub> at 300°C [9], the formation rate of hydrocarbons from CO<sub>2</sub> in our study was significantly lower than that from CO partly because of the low formation rate of CO under the reaction conditions. The surface oxidation state of the catalyst reduced at 500°C after the reaction with CO<sub>2</sub> is similar to that for the catalyst reduced at 350°C after the reaction with CO (cf. Fig. 6c and e). However, the product distribution of the reaction with CO<sub>2</sub> is significantly different from that for the reaction with CO, suggesting that

the surface oxidation state does not seriously affect the nature of the active sites. Accumulation of carbon and oxygen was observed over iron foil in the reaction with CO<sub>2</sub> [9], suggesting that active carbide species is formed on the surface. Hence, formation of carbide and oxide probably occurs on the metallic surface of the iron catalyst reduced at 500°C during the activation process in the reaction with CO<sub>2</sub>. The very slight peak at 41.8° may be attributed to  $\chi$ -Fe<sub>2.2</sub>C, suggesting the presence of the carbide species. In the presence of CO<sub>2</sub>, elimination of carbide readily takes place to form CO and suppresses the formation of the active carbide species. Consequently, the surface concentration of carbide species is lower in the case of the reaction with CO<sub>2</sub>. It is reasonable to say that the lower concentration of the active sites results in small probability of chain growth and increases the chance of hydrogenation. Although carbide species can be formed readily on the surface of Fe<sub>3</sub>O<sub>4</sub>, the activation of the catalyst reduced at 350°C was slow. The XPS analyses show that the surface of the catalyst is oxidized after the reaction, suggesting that the surface is close to that of Fe<sub>2</sub>O<sub>3</sub> whose activation is very gradual [3].

## 5. Conclusions

When the major phase of the iron catalyst is Fe<sub>3</sub>O<sub>4</sub>, active carbide species are readily formed on the surface as well as on the metallic iron during the reaction with CO. Simultaneously, reduction of the surface oxide to metal takes place. On the other hand, oxidation of the surface iron proceeds during the reaction with CO<sub>2</sub>, and a slight quantity of carbide species is formed on the surface. The formation of active carbide species may be suppressed in presence of CO<sub>2</sub> to give CO. Hence, the concentration of the active carbide species is lower in the reaction with CO<sub>2</sub> than in CO reaction, and the lower concentration results in (i) lower space–time yield of hydrocarbons, (ii) higher selectivity to

light hydrocarbons, and (iii) higher paraffin selectivity in the products.

## References

- [1] S. Soled, E. Iglesia, R.A. Fiato, *Catal. Lett.* 7 (1990) 271.
- [2] D.B. Bukur, D. Mukesh, S.A. Patel, *Ind. Eng. Chem. Res.* 29 (1990) 194.
- [3] R.A. Dictor, A.T. Bell, *J. Catal.* 97 (1986) 121.
- [4] M.E. Dry, in: J.R. Anderson, M. Boudart (Eds.), *Catalysis Science and Technology 1* Springer, New York, 1982, p. 159.
- [5] J.P. Reymond, P. Mériaudeau, S.J. Teichner, *J. Catal.* 75 (1982) 39.
- [6] F. Blanchard, J.P. Reymond, B. Pommier, S.J. Teichner, *J. Mol. Catal.* 17 (1982) 171.
- [7] R.J. Madon, W.F. Taylor, *J. Catal.* 16 (1981) 32.
- [8] G.B. Raupp, W.N. Delgass, *J. Catal.* 58 (1979) 361.
- [9] D.J. Dwyer, G.A. Somorjai, *J. Catal.* 52 (1978) 291.
- [10] D. Miller, M. Moskovits, *J. Am. Chem. Soc.* 111 (1989) 9250.
- [11] H. Ando, Q. Xu, M. Fujiwara, Y. Matsumura, M. Tanaka, Y. Souma, *Catal. Today* 45 (1998) 229.
- [12] G. Kishan, M.-W. Lee, S.-S. Nam, M.-J. Choi, K.-W. Lee, *Catal. Lett.* 56 (1998) 215.
- [13] P.H. Choi, K.-W. Jun, S.-J. Lee, M.-J. Choi, K.-W. Lee, *Catal. Lett.* 40 (1996) 115.
- [14] J.-F. Lee, W.-S. Chern, M.-D. Lee, T.-Y. Dong, *Can. J. Chem. Eng.* 70 (1992) 511.
- [15] M.-D. Lee, J.-F. Lee, C.-S. Chang, *Bull. Chem. Soc. Jpn.* 62 (1989) 2756.
- [16] M. Pijolat, V. Perrichon, M. Primet, P. Bussière, *J. Mol. Catal.* 17 (1982) 367.
- [17] H.P. Klug, L.E. Alexander, *X-ray Diffraction Procedures*, John Wiley and Sons, New York, 1954.
- [18] C.D. Wagner, W.M. Riggs, L.E. Davis, J.F. Moulder, in: G.E. Muilenberg (Ed.), *Handbook of X-ray Photoelectron Spectroscopy*, Perkin-Elmer, Minnesota, 1978.
- [19] JCPDS powder diffraction files: 6-696, 19-629.
- [20] J.A. Amelse, J.B. Butt, L.H. Schwartz, *J. Phys. Chem.* 84 (1980) 3363.